

# COMPUTER AIDED CLASSIFICATION OF CERAMICS

**Martin Kampel**

Pattern Recognition and Image Processing Group  
Institute for Automation, Technische Universität Wien, AUSTRIA

**Robert Sablatnig**

Pattern Recognition and Image Processing Group  
Institute for Automation, Technische Universität Wien, AUSTRIA

*Every archaeological excavation must deal with a vast number of ceramic fragments. The documentation, administration and scientific processing of these fragments represent a temporal, personnel, and financial problem. Up to now documentation and classification have been done manually which means a lot of routine work for archaeologists and a very inconsistent representation of the real object. First, there may be errors in the measuring process. (Diameter or height may be inaccurate), second, the drawing of the fragment should be in a consistent style, which is not possible since a drawing of an object without interpreting it is very hard to do.*

*We are developing a documentation system for archaeological fragments based on their profile, which is the cross-section of the fragment in the direction of the rotational axis of symmetry. Hence the position of a fragment (orientation) on a vessel is important. To achieve the profile, a 3D-representation of the object is necessary. The main technical goal of this project is to perform an automated classification and reconstruction of archaeological fragments by using the profile section of the oriented object and additional attributes (type of clay, dimensions, type of vessel and the site) belonging to the fragment. The final aim is to provide a tool that helps archaeologists in their archivation process. This paper gives an overview about an automated archivation process and 3D-acquisition with respect to archaeological requirements.*

## 1. INTRODUCTION

Ceramics are one of the most widespread archaeological finds and are a short-lived material. This property helps researchers to document changes of style and ornaments. Therefore, ceramics are used to distinguish between chronological and ethnic groups. Furthermore ceramics are used in the economic history to show trading routes and cultural relationships. Especially ceramic vessels, where shape and decoration are exposed to constantly changing fashion, not only allow a basis for dating the archaeological strata, but also provide evidence of local production and trade relations of a community as well as the consumer behaviour of the local population (ORTON, TYERS and VINCE 1993).

In order to make a later classification possible, the object is described in different ways: shape, decoration, technological manufacturing stage, material, and colour. Shape is usually described in terms of type-series using traditional pottery classification systems. For this, the description of the profile is important. Decoration, material, colour, and a careful examination of the traces left on the vessel which indicate the steps taken during the manufacturing process is a further important property to be investigated in order to perform a subsequent classification. The purpose of classification is to get a systematic view of the material found (if every piece would be treated as unique, this would immediately lead to the wood-for-the-trees syndrome due to the vast amount of information), to recognize types, and to add labels for additional information as a measure of quantity. It is used to relate a fragment to existing parts in the archive. The colour information is very important in the pre-classification process since archaeologists use this colour information to

relate a fragment to an excavation layer, age, manufacture, or even to a certain pot. The classification of fragments can be divided into two main parts: shape features and properties.

The *classification of shape* defines the process where archaeologists distinguish between various features, like the profile (KAMPEL and SABLATNIG 1999), the dimensions of the object, like diameter, and the type of surface (MENARD and SABLATNIG 1996), whereas the *classification of material* copes with different characteristics of a fragment like the clay, the colour (KAMPEL and SABLATNIG 2000) and the surface properties.

The paper is organized as follows: In Section 1 we describe how we model complete objects using shape from silhouette, in Section 2 the 3D reconstruction of fragments is explained. A laser range sensor is described in Section 4. In Section 5 we present a method for colour calibration. Experimental results are described for each section and we conclude with a summary and outline.

## 2. SHAPE FROM SILHOUETTE FOR 3D MODELING OF COMPLETE OBJECTS

Shape from Silhouette is a method of automatic construction of a 3D model of an object based on a sequence of images of the object taken from multiple views, in which the object's silhouette represents the only interesting feature of an image (SZELISKI 1993, POTSEMI 1987). The object's silhouette in each input image corresponds to a conic volume in the object real-world space (see Figure 1). A 3D model of the object can be built by intersecting the conic volumes from all views. Shape from Silhouette is a computationally simple algorithm – it employs only basic matrix operations for all

transformations – and it requires only a camera as equipment, so it can be used to obtain a quick initial model of an object which can then be refined by other methods. It can be applied on objects of arbitrary shapes, including objects with certain concavities (like a handle of a cup), as long as the concavities are visible from at least one input view. It can also be used to estimate the volume of an object. The shape from Silhouette algorithm used is described in detail in (TOSOVIC 2000).

The acquisition system (KAMPEL and TOSOVIC 2000) consists of the following devices:

- a monochrome CCD-camera with a focal length of 16 mm and a resolution of  $768 \times 576$  pixels
- a turntable with a diameter of 50 cm, whose desired position can be specified with an accuracy of 0.05 degrees.

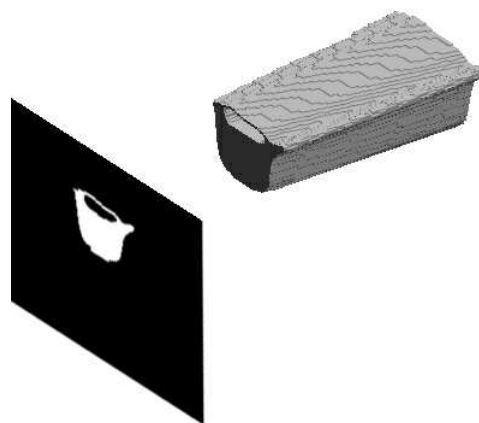


Figure 1. Image silhouette and the corresponding conic volume.

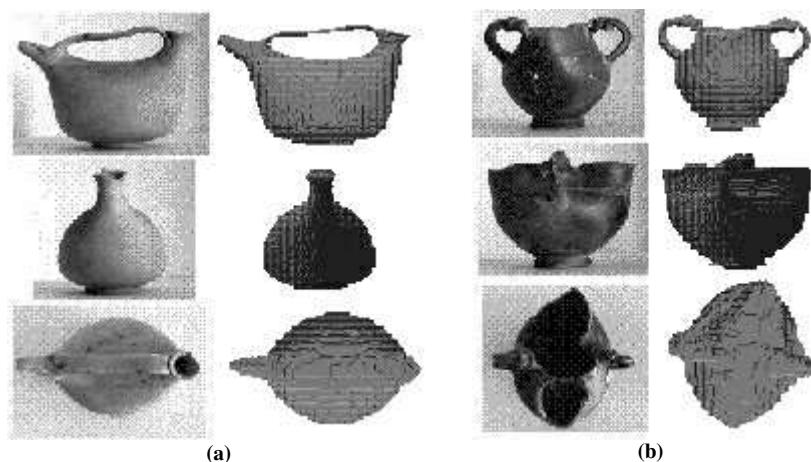


Figure 2. Constructed models of real objects in different voxel resolution.

An important issue is the illumination of the object observed, which should be clearly distinguishable from the background, independent from the object's shape or the type of its surface. For that reason back-lighting (HARALICK and SHAPIRO 1991) is used. A large (approx.  $50 \times 40$  cm) rectangular lamp is put behind the turntable (as seen from the camera). In addition, a white piece of paper, larger than the lamp, is put right in front of the lamp, in order to make the light more diffuse. The whole system is protected against the ambient light by a thick black curtain.

Prior to any acquisition, the system is calibrated in order to determine the inner and outer orientation of the camera and the rotational axis of the turntable. The calibration method used was exclusively developed for the Shape from Silhouette algorithm used and it is described in detail in (TOSOVIC 1999) and (KAMPEL and TOSOVIC 2000).

Figure 2 shows the reconstructed 3D models of the two pots from three sides. For these models octree resolution of  $256^3$  voxels was built, based on input images from 36 views. The results with both synthetic and real input data show that there is a certain minimal octree resolution required to obtain an accurate model of an object, especially for highly detailed objects, like the two pots used for tests with real images. Concerning the number of input views used for obtaining a model of an object, it turned out that beginning from 12 views, the constructed model does not change significantly. In our tests the octrees built from 12 views were almost the same as the ones built from 36 views, except that they took much less time to construct.

The results with synthetic data, where we had a perfect

transformation matrix, showed that the error in the dimensions of the model lies within or is slightly higher than the error introduced through the minimal voxel size. The error with real data depends additionally on the accuracy of the calibration algorithm. The results also showed that the algorithm works much better with oval objects, i.e., with objects that do not have completely flat surfaces or sharp edges.

### 3. CODED LIGHT FOR 3D RECONSTRUCTION OF FRAGMENTS

Our documentation system for archaeological fragments is based on the profile, which is the cross-section of the fragment in the direction of the rotational axis of symmetry. Hence the position of a fragment (orientation) on a vessel is important. To achieve the profile, a 3D-representation of the object is necessary.

Archaeological pottery is assumed to be rotationally symmetric since it was made on a rotation plate. With respect to this property the axis of rotation is calculated using a Hough inspired method (BEN-JACOUB and MENARD 1997). To perform the registration of the two surfaces of one fragment, we use a-priori information about fragments belonging to a complete vessel: both surfaces have the same axis of rotation since they belong to the same object.

Figure 3 gives an overview of a 3D-surface reconstruction from two object views. The first step consists of sensing the front- and backside of the object (in our case a rotationally

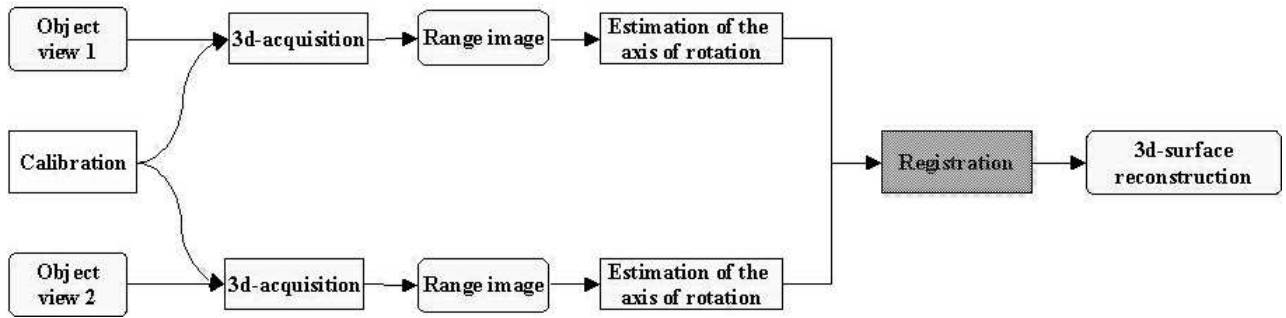


Figure 3. 3D surface reconstruction overview.

symmetric fragment) using a calibrated 3D-acquisition system. We register the resulting range images by calculating the axis of rotation of each view and bringing the estimated axes into alignment. The method is described in detail in (KAMPEL 1999).

In our acquisition system the stripe patterns are generated by a computer controlled transparent Liquid Crystal Display (LCD 640) projector. The light patterns allow the distinction of 2<sup>n</sup> projection directions. Each direction can be described uniquely by a n-bit code. A CCD-camera is used for acquiring the images.

The projector projects stripe patterns onto the surface of the objects. In order to distinguish between stripes they are binary encoded. The camera grabs gray level images of the distorted light patterns at different times. With the help of the code and the known orientation parameters of the acquisition system, the 3D-information of the observed scene point can be computed. This is done by using the triangulation principle.

The image obtained is a 2D array of depth values and is called a range image (Figure 4).

To find out if the method is working on real data we used

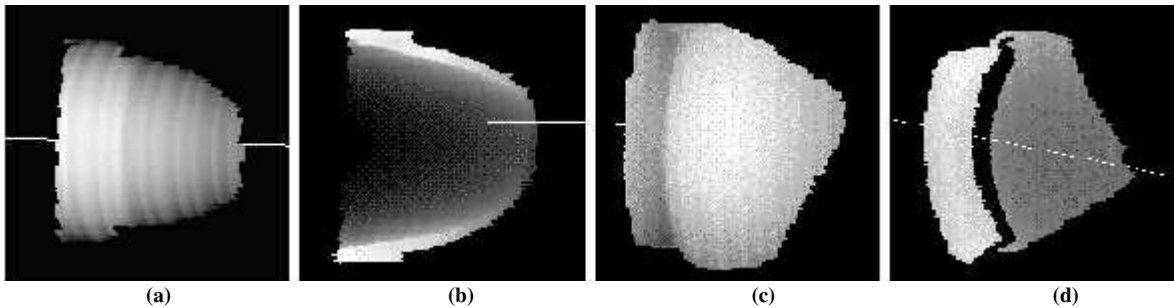


Figure 4. Front- and back-view (range images) and their axis of rotation of a flowerpot (a, b) and an archaeological fragment (c, d).

a totally symmetric small flowerpot with known dimensions and took a fragment which covered approximately 25% of the original surface. The range images of the front- and back-view consisted of approximately 10.000 surface points each (Figure 4a, 4b). The mean distance  $d$  between the surfaces is 5.64 mm and the

registration error  $\delta = 1.42$  mm. The distribution of the registration error delta for the flowerpot is shown in Figure 5a. The registration error increases towards the top of the pot, because of the irregularity of the distance between the surfaces at that region since the flowerpot has an edge (upper border) where inner and outer surface are not parallel.

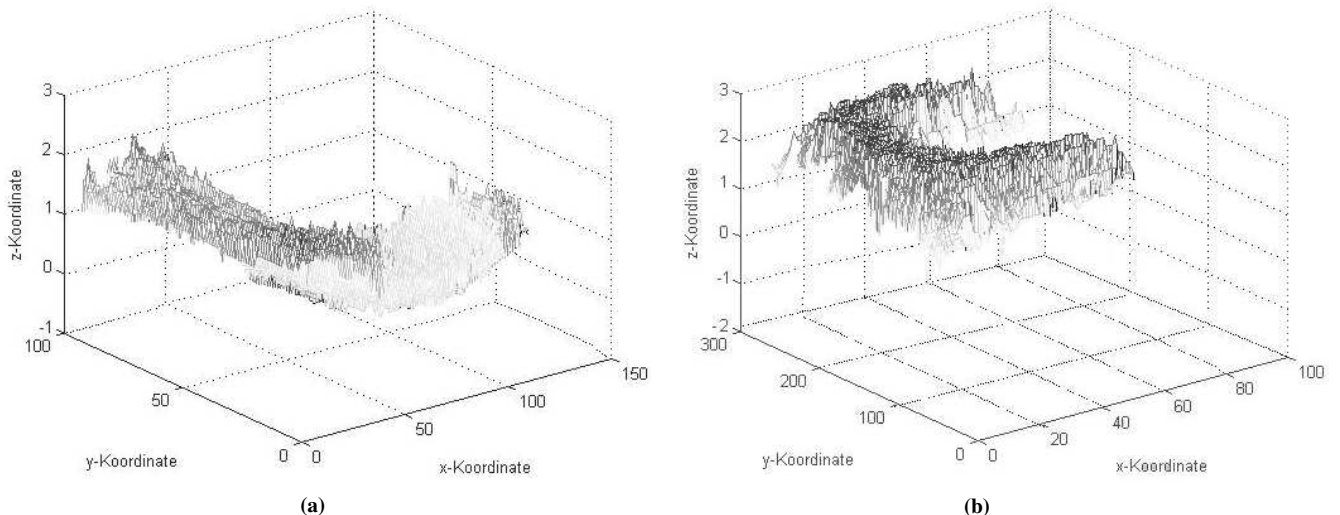


Figure 5. Distribution of  $d$  for registered flowerpot (a) and archaeological fragment (b).

Figure 4c and d show the front-view, back-view and the axis of rotation of a real archaeological fragment. Registration tests with this fragment resulted in registration errors of approximately  $\delta = 1.7\text{mm}$  and a mean distance of  $d = 5.8\text{mm}$ .

Figure 5b shows the distribution of  $\delta$  of a registered archaeological fragment. Marginal peaks are caused by shadow regions of the back-view (see Figure 4d) at the border of the fragment, where either no range data is

processed or the range information is unreliable. The increase of the registration error  $\delta$  reflects the uneven surface of the fragment.

Further problems that arise with real data are symmetry constraints, i.e. if the surface of the fragment is too flat or too small, the computation of the rotational axis is ambiguous (worst case: sphere) which results in sparse clusters in the Hough-space which indicate that the rotational axis is not determinable.

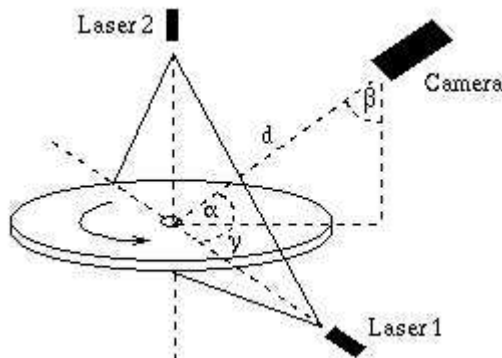
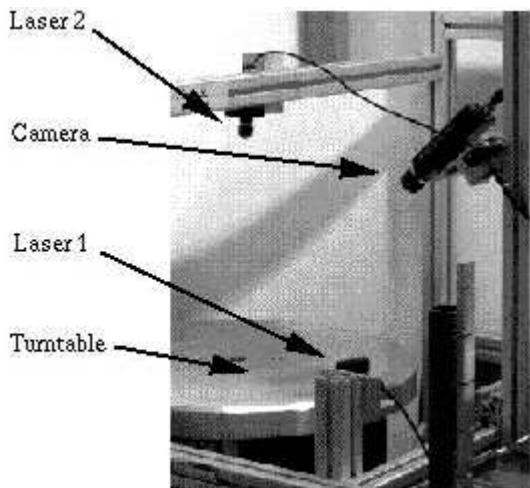


Figure 6. Acquisition system.

#### 4. LASER RANGE SENSOR

The acquisition method used for estimating the 3D-shape of objects is shape from structured light, based on active triangulation (DE PIERO and TRIVEDI 1996). The camera is positioned between the two lasers facing the measurement area. The complete system consists of

- 1 turntable with a diameter of 50 cm, which can be rotated about the z-axis, used to move the object of interest through the acquisition area.
- 2 red lasers to illuminate the scene, one mounted on the top (distance to rotation plane is 45 cm), one beside the turntable (distance to the rotation center is 48 cm). Both lasers are extended with cylindrical lenses to spread the laser beam into one illuminating plane. The laser light

plane intersects with the object surface, forming one laser stripe.

- 1 CCD-camera (b/w) with a 16 mm focal length, a resolution of 768x572 pixels, and a distance of 40 cm to the rotation center. The angle between the camera normal vector and the rotation plane is approx. 45 degrees. A frame grabber card is used to connect the camera to a PC.
- 1 Intel Pentium PC under Linux operating system.

Figure 6 depicts the complete hardware setup (a) and its geometric arrangement (b).

An iterative process for 3D surface reconstruction in static environments is defined by the following steps, which depicts this process

- Image acquisition: The scene is captured by the CCD-

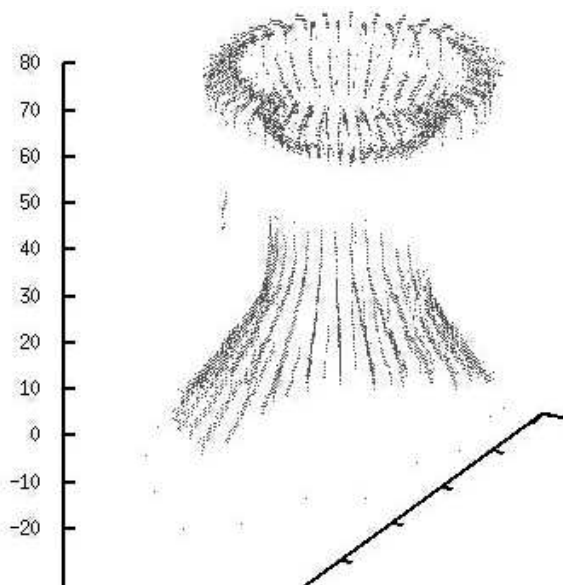


Figure 7. Reconstruction of pottery.

camera. The result is a greyscale- image which shows the intersection between the laser plane and the object which is a line.

- Feature extraction: The line shown in the camera image is extracted. The result is a set of 2D points.
- Registration: The set of 2D points extracted in the previous step is transformed from the world coordinate system in its object coordinates.
- Integration: Each registered point is integrated into the existing model computed and integrated at the previous iterations of the acquisition process.
- Next View Planning: The next viewing angle is computed based on the algorithm shown in the previous section and the turntable moves to the calculated absolute angle. The process repeats until the turntable revolves one complete rotation.
- 3D-model visualization of the reconstructed surface.

Figure 7 shows the reconstruction of the head of an amphora after the acquisition process. The chosen angles are between 4 and 12 degrees. The analysis of the reconstruction data shows that the axis of symmetry is switched from the center of rotation by 1.8 mm in x-direction and 2.1 mm in y-direction. In order to scan the whole image 36 steps were necessary. Figure 2b shows the rendered object after the surface reconstruction process. The visualization results from a modified z-buffer-algorithm.

## 5. COLOUR ESTIMATION

Archaeologists determine the specific colour of a fragment by matching it to the Munsell colour patches (MENARD and TASTL 1996, WYSZECHI and STILES 1982). Since this process is done "manually" by different archaeologists and under varying light conditions, the results differ from each other. In general, photos of fragments are taken in order to have colour representations in the archive. Due to different camera characteristics and changing light conditions the colour of a fragment in images varies.

We propose a solution to the colour classification assuming that the spectral reflectance of archaeological fragments varies slowly in the visible spectrum. We present an approach for accurate colourimetric information on fragments, performed on digital images containing

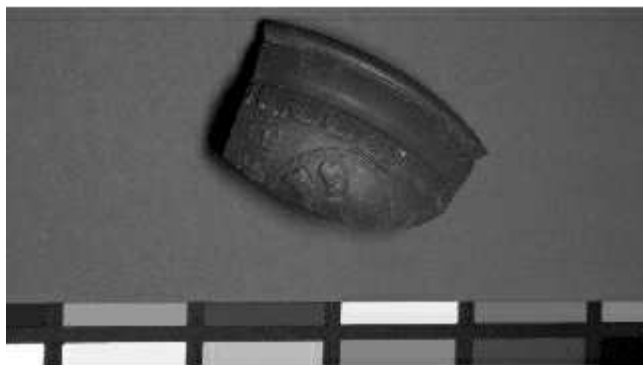


Figure 8. Archaeological fragment together with MacBeth colour checker.

archaeological fragments under different illuminants with a priori known spectral illumination. A characteristic vector analysis (SIMONDS 1963) of the reference reflectance leads to an algorithm that computes the colourimetrically accurate reflectance out of a video digitizing system.

In order to provide a device-independent colour specification we use reference colours from the MacBeth Colour chart (MCCAMY, MARCUS and DAVIDSON 1976). Figure 8 shows a fragment together with parts of the MacBeth rendition chart.

Our approach rests upon Lee's method (LEE 1988) assuming that spectral illumination is known and that the spectral reflectance of our material varies slowly in the visible spectrum. This means that small changes of RGB values should lead to small changes in reflectance. Prior knowledge about the illuminant leads to chromaticity and luminance information.

Each RGB pixel in a digitized image has a value proportional to weighted integral over the visible spectrum. This integral depends on three spectral variables. This is the spectral irradiance  $E(\lambda)$ , which describes the energy per second at each wavelength  $\lambda$ . The proportion of light of wavelength  $\lambda$  reflected from an object is determined by the surface spectral reflectance  $S(\lambda)$ . We assume that there are  $k$  distinct channels in the digitizing system and use  $k = 3$  for red, green and blue. We denote the spectral response of the  $k^{\text{th}}$  channel as  $R_k(\lambda)$  and a pixel value for the  $k^{\text{th}}$  colour channel as  $p_k$ .

$$p_k = \int S(\lambda)E(\lambda)R_k(\lambda)d(\lambda) \quad \text{Eq 1}$$

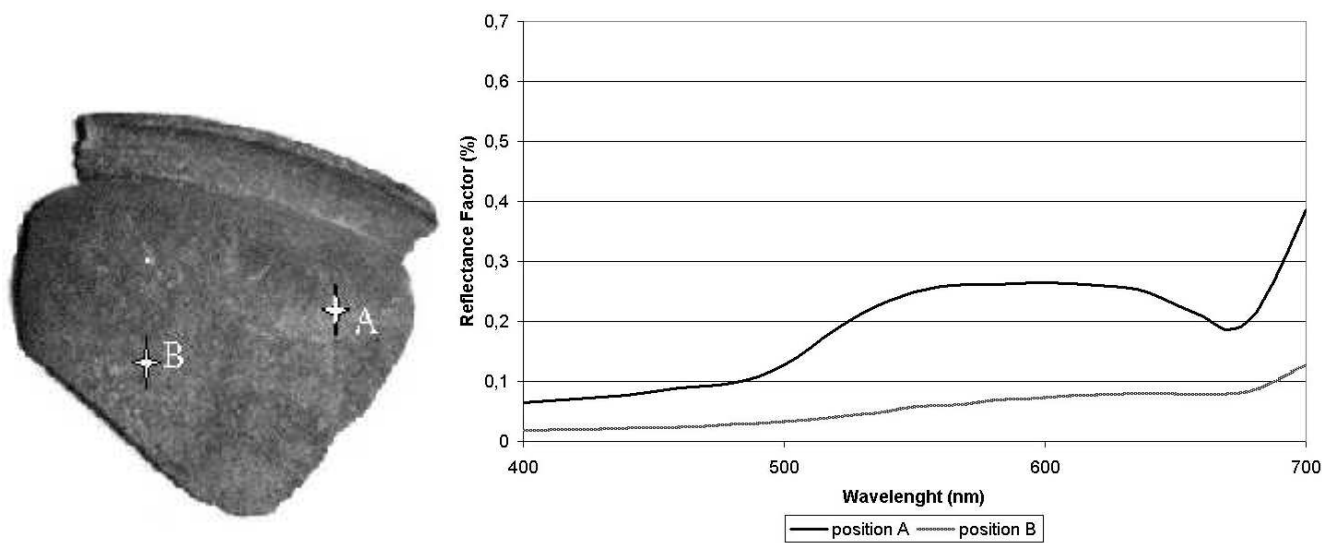


Figure 9. Test regions of a sherd and their spectral reflectance.

Eq 1 describes the relationship between pixel values and spectral quantities. We approximate the three integrals above as summations over wavelength, using values every 10nm in the visible spectrum from 400nm to 700nm. If the proportionality factor in the  $R_k(\lambda)$  is subsumed, one can construct the following matrix equation (Eq. 2).  $m$  denotes the steps to be taken in the spectrum.

$$p = SER \quad \text{Eq 2}$$

- $p$  1 by 3 row vector (RGB)
- $S$  1 by  $m$  row vector (surface reflectance)
- $E$   $m$  by  $m$  diagonal matrix (spectral irradiance)
- $R$   $m$  by 3 matrix (system spectral transfer function)

Since only an approximated knowledge of the system function  $R$  is assumed, the goal will be to:

- specify the system transfer function  $R$  more accurately by analyzing colour samples with known reflectance of the MacBeth Colour patches.
- use this new information to find the unknown spectral reflectance of other samples illuminated by the same light source.

For a more detailed description of the algorithm see (Lee 1988).

As an experiment we grab an image of a fragment and specify two test regions A and B (Figure 9a). The spectral reflectances of A and B are computed and visualized in figure 9b. For evaluation purposes we calculate CIE tristimulus values using a linear transformation and compare the achieved values with measured chromaticity coordinates from a Chroma Meter CR-200b. The final results are in the close neighborhood of the measured values. Since these results are influenced by the linear transformation, we plan measurements using a spectroradiometer, in order to allow direct comparison between measured and computed reflectances.

## 6. CONCLUSION AND OUTLOOK

We have proposed a prototype system for 3D acquisition of archaeological fragments. The work was performed in the framework of the documentation of ceramic fragments. We also presented a technique for accurate colour estimation, which plays an important role in the classification process for archaeological pottery.

The methods proposed have been tested on synthetic and real data with reasonably good results. It is part of continuing research efforts to apply the 3D data achieved in order to identify fragments of the same object. Future work also goes towards colour calibration without known illuminants in order to allow colour estimation outside laboratory conditions.

## ACKNOWLEDGEMENTS

This work was supported by the Austrian Science Foundation (FWF) under grant P13385-INF.

## BIBLIOGRAPHY

BEN-YACOB, S., MENARD C., 1997. *Robust Axis Determination for Rotational Symmetric Objects out of Range Data*. In W. Burger and M. Burge (eds.) *21st Workshop of the OEGAM*, 197-202, Hallstatt, Austria, May 1997.

DE PIERO, F. and TRIVEDI, M., 1996. *3-D computer vision using structured light: Design, calibration, and implementation issues*. *Advances in Computers*, 43, 243-278.

HARALICK, R.M. and SHAPIRO, L.G., 1991. *Glossary of computer vision terms*. *Pattern Recognition*, 24 (1), 69-93.

KAMPEL, M., 1999. *Tiefendatenregistrierung von rotationssymmetrischen Objekten*, Master Thesis, Vienna University of Technology, Institute of Automation.

KAMPEL, M. and SABLATNIG, R., 1999. *On 3D Modelling of Archaeological Sherds*. In *Proceedings of International Workshop on Synthetic-Natural Hybrid Coding and Three Dimensional Imaging*, 95-98.

KAMPEL, M. and SABLATNIG, R., 2000. *Colour Classification of Archaeological Fragments*. In *Proc. of the 15th International Conference on Pattern Recognition*, vol. 4, 771-774.

KAMPEL, M. and TOSOVIC, S., 2000. *Turntable Calibration for automatic 3D-Reconstruction*. In *Applications of 3D-Imaging and Graph-based Modelling*, Proceeding of the 24th Workshop of the Austrian Association for Pattern Recognition (OEGAM), 25-31.

KLETTE, R., KOSCHAN, A. and SCHLÜNS, K., 1993. *Computer Vision. Räumliche Information aus digitalen Bildern*. Vieweg Verlag, Braunschweig/Wiesbaden 1996.

LEE, R.L., 1988. *Colourmetric calibration of a Video Digitizing System*. *Colour Research and Application*, 13 (3), 180-186.

MALONEY, L.T. and WANDELL, B.A., 1986. *Colour Constancy: a method for recovering surface spectral reflectance*. *Journal of the Optical Society of America*, vol 3 (1), 29-33.

MCCAMY, C.S., MARCUS, H. and DAVIDSON, J.G., 1976. *A Colour-Rendition Chart*. *Journal of Applied Photographic Engineering*.

MENARD, C. and SABLATNIG, R., 1996. *Computer based Acquisition of Archaeological Finds: The First Step towards Automatic Classification*. In H. Kamermans and K. Fennema, (eds.), *Interfacing the Past, Computer Applications and Quantitative Methods in Archaeology*, *Analecta Praehistorica Leidensia*28, 413-424.

MENARD, C. and TASTL, I., 1996. *Automated Colour Determination for Archaeological Objects*. In *Is&T Fourth Colour Imaging Conference*, Scottsdale, 160-163.

ORTON, C., TYERS, P. and VINCE, A., 1993. *Pottery in Archaeology*. Cambridge, Cambridge University Press.

POTSEMIL, M., 1990. *Generating octree models of 3D objects from their silhouettes in a sequence of images*. *Computer Vision, Graphics, and Image Processing*, 40, 68-84.

SIMONDS, J.L., 1963. *Application of characteristic vector analysis to photographic and optical response data*. *Journal of the Optical Society of America*, 53, 968-974.

SZELISKI, R., 1993. *Rapid octree construction from image sequences*. *CVGIP: Image Understanding*, 58(1), 23-32, July 1993.

TOSOVIC, S., 1999. *Lineare Hough-Transformation und Drehtellerkalibrierung*, Technical Report, PRIP-TR-59, Pattern Recognition and Image Processing Group, Institute for Computer Aided Automation, Vienna University of Technology.

TOSOVIC, S., 2000. *Shape from Silhouette*, Technical Report, PRIP-TR-64, Pattern Recognition and Image Processing Group, Institute for Computer Aided Automation, Vienna University of Technology.

WYSZECHI, G., STILES, W.S., 1982. *Colour Science: Concepts and Methods, Quantitative Data and Formula*, New York, John Wiley and Sons, 2nd edition.